CHEMISTRY
A EUROPEAN JOURNAL

DOI: 10.1002/chem.201001167

# Surface Passivation-Induced Strong Ferromagnetism of Zinc Oxide Nanowires

**Shu-Ping Huang, Hu Xu, Igor Bello, and Rui-Qin Zhang*[a]**

II–VI semiconducting materials have attracted much interest owing to their potential applications in spintronics,[1a] light-emitting diodes,[1b] and laser diodes.[1c] Of these materials, ZnO has become a recent focus because of its novel electronic, optical, and magnetic properties, which facilitate the creation of multifunctionally integrated devices in a single monolithic structure. In particular, ZnO nanosized structures offer added property values associated with nanostructures that are greatly influenced by their diameters, crystallographic orientations, surface passivation, presence of dopants, and so forth. The bare and completely passivated wires are semiconducting, and the band gap of ZnO nanowires (ZnONWs) can be tuned by changing the wire diameter and by using different surface passivants.[2–3] In spintronic applications, the ultimate goal of research is the development of ferromagnetic ZnO at room temperature. The primary method for introducing magnetism into ZnO is doping with a small amount of transition metals (TMs).[4] However, debates have arisen over the origin of magnetism in TM-doped ZnO because magnetic TMs are intrinsically magnetic and their precipitates or secondary magnetic phases in the host semiconductor may be the primary cause of the observed ferromagnetism. The dispute over the presence of magnetic precipitates can be solved by introduction of a new type of dilute magnetic semiconductor (DMS). Although ferromagnetism in N- or C-doped ZnO and ZnO with intrinsic point defects (e.g., a Zn vacancy) have been explored experimentally[5a–c] and theoretically,[5b,d–g] the poor controllability and destructive processing due to volume doping impose an inherent disadvantage. Surface passivation doping[6] has been shown to be an alternative approach to conventional volume doping for modulating the conductivity of silicon nanowires. Interestingly, some recent experimental[7a,d–e] and theoretical[7b–e] studies report that the magnetic properties of ZnO may also be induced by surface effects, which indicate the importance of the surface of low-dimensional ZnO. Among them, Garcia et al.[7a] experimentally prove that the adsorption of certain organic molecules onto the surface of ZnO nanoparticles modifies their electronic structure and gives rise to ferromagnetic-like behavior at room temperature. However, most of these studies focus on nanoparticle systems in which the surfaces are multifaceted; the lack of long-range ordering leads to poor control over the magnetic properties.[7e] One-dimension single-crystalline ZnONWs, on the other hand, possess a large surface-to-volume ratio, well-defined facets on the surface, and an anisotropic geometry for the shape-tunable magnetic properties.[7e] Most recently, experimental magnetic moments and room-temperature ferromagnetism in thiol-capped ZnONW or nanotube arrays have been reported; it was found that the magnetic moments can be varied by changing the length of the nanowires.[7e] But again the underlying mechanism of ferromagnetism remains largely unsolved. Also, what is the effect of other capped species, such as F, Cl, OH, and $NH_2$? These small inorganic species should have smaller steric hindrance effects than organic molecules on the surfaces and thus could more efficiently alter the system magnetic moments. A study of these surface terminates could also elucidate the effect of their electronegativity on the distribution of magnetic moments.

In addition, the half-metallic (HM) characteristic of ZnO, in which the conduction electrons at the Fermi energy $E_F$ are fully spin polarized, would also be desirable to study. HM materials are ideal for spintronic applications, such as the tunneling of magnetoresistance and giant magnetoresistance elements. The HM density of states (HMDOS) at $E_F$ of $Co_xZn_{1-x}O$ was predicted by using theoretical approaches within density functional theory (DFT),[8] but DFT+$U$ calculations[9a] showed they were just magnetic semiconductors, consistent with the poor conductivity in experiments.[9b] The recent DFT study by Chen et al.[10] demonstrates that zigzag

[a] Dr. S.-P. Huang, Dr. H. Xu, Prof. I. Bello, Prof. R.-Q. Zhang
Center of Super-Diamond and Advanced Films and
Department of Physics and Materials Science
City University of Hong Kong
Hong Kong SAR (P.R. China)
Fax: (+852) 3442-0538
E-mail: aprqz@cityu.edu.hk

Supporting information for this article is available on the WWW under http://dx.doi.org/10.1002/chem.201001167.

ZnO nanoribbons (constructed from stable graphitic-like sheets) can show HM behavior by $NH_2$ edge passivation. The problem is still open because a DFT+$U$ study might destroy the HM state. Even the results obtained with DFT+$U$ have to be regarded with caution.[11] Opportunities remain for ZnONWs to present HM properties, in particular when passivants of large electronegativity are adopted.

In this work, we show theoretically inducing half-metal characteristics of ZnONWs by surface saturation of only the zinc dangling bonds (DBs) with fluorine using both DFT and DFT+$U$ calculations. This result is significant to solve the dispute on the origin of magnetic properties, while it also poses a possible route for fabrication of HM ZnONWs by the sole manipulation of NWs surfaces.

We chose triangular, quadrangular, and hexangular ZnONWs along the $<0001>$ direction enclosed by $(10\bar{1}0)$ facets for study, and constructed their initial atomic configurations from the bulk wurtzite structure. X-ZnO $(10\bar{1}0)$ or X-ZnONW denote a ZnO $(10\bar{1}0)$ surface or nanowire with all Zn DBs on the surface passivated by chemical species X after relaxation (X = F, Cl, OH, and $NH_2$). For the hexangular F-ZnONW, we also considered that only half of the Zn DBs is passivated by F (6 F atoms/unit cell) in two different configurations. One configuration involves each second layer of Zn DBs being passivated, denoted as F-ZnONW-1. There are two Zn-O dimer layers along the wire direction in a unit cell of ZnONW. In the second configuration, labeled F-ZnONW-2, each alternate Zn DB is passivated.

We first present the optimized structures, and the results show that the chemical species F, Cl, OH, and $NH_2$ energetically favor adsorption on the Zn surface sites instead of the O surface sites. The detailed total energy comparison for the various adsorption sites of F, Cl, OH, and $NH_2$ are provided in the Supporting Information. F-ZnONW-2 is 494 meV energetically more favorable than F-ZnONW-1, which may be due to the larger repulsion of F atoms in F-ZnONW-1. Figure 1 depicts the relaxed structures of the F-, HO-, and $H_2N$-ZnO $(10\bar{1}0)$ surfaces and the relaxed structures of hexangular F-ZnONWs, F-ZnONW-1, and F-ZnONW-2. For F-ZnO $(10\bar{1}0)$, the surface oxygen atoms located in the first layer relax toward the bulk region, whereas the corresponding zinc atoms relax outwards due to the strong attraction of F. For the Cl-, OH-, and $NH_2$-ZnO $(10\bar{1}0)$ surfaces, the surface oxygen atoms located in the first layer relax slightly toward the bulk region, whereas the corresponding zinc atoms remain close to their bulk positions owing to the close electronegativities of N, Cl, and O. There are intra-molecular hydrogen bonds in the $H_2N$- and HO-ZnO $(10\bar{1}0)$, and the N-H···O(s)-Zn(s) and O-H···O-H lengths are 2.13 and 2.46 Å, respectively. The lengths of the surface Zn–O bonds parallel to the axis are 1.87, 1.90, 1.90, and 1.93 Å for F-, Cl-, HO-, and $H_2N$-ZnONWs, respectively, which are closer to that of the bulk ($\approx$2.0 Å) when compared to the bond length in bare wires (1.82 Å). The Zn–O bond lengths and angles in the core of the NWs are less affected and are close to the bulk ZnO values, which indicates the localized effect of passivation.

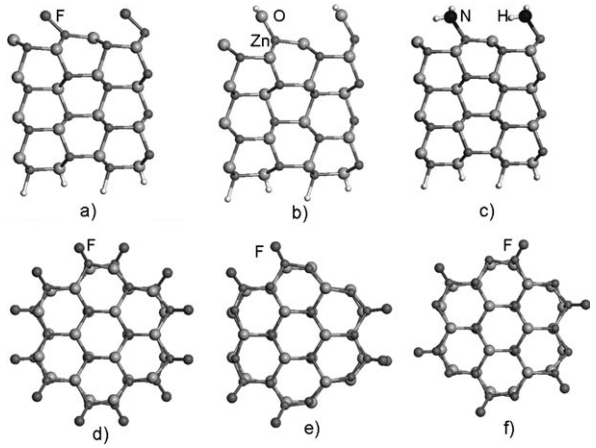


Figure 1. Side view of X-ZnO $(10\bar{1}0)$: a) F-ZnO $(10\bar{1}0)$, b) HO-ZnO $(10\bar{1}0)$, and c) $H_2N$-ZnO $(10\bar{1}0)$; the bottom surface DBs are saturated by pseudo hydrogen atoms, and only the Zn DBs of the top surface are passivated. Top views of hexangular d) F-ZnONW, e) F-ZnONW-1 (each second layer of the Zn DBs is saturated), and f) F-ZnONW-2 (each alternate Zn DB is saturated).

To verify the energetic stability of the passivated wires, in the following we calculate the corresponding adsorption energies (see Tables S3 and S4 in the Supporting Information). All the adsorption energies are negative, indicating that all the studied adsorptions are exothermic and should be observed in experimental work. The 25 or 50% passivation is energetically more favorable than full passivation. The adsorption energy of F on ZnONW surfaces attained the largest absolute value at half passivations, which implies the easiest formation of F-ZnONWs.

To obtain the ground-state structures, we used different initial guesses for the magnetic moment locations of X-ZnO $(10\bar{1}0)$ surfaces and F-ZnONWs, including ferromagnetic (FM), anti-ferromagnetic (AFM), and nonmagnetic (NM) spin configurations. Several possible AFM-ordered structures were considered for the AFM state. The calculations show that the ground states of bare ZnONWs and $(10\bar{1}0)$ surfaces with both Zn and O DBs have no magnetism, which is consistent with experimental results,[8c] and that the non-dissociative $NH_3$ adsorption on $(10\bar{1}0)$ surface of Zn sites does not induce magnetism neither. The ferromagnetic property of O-terminated ZnO (0001) surfaces with adsorbed $NH_3$[8b] is mainly the intrinsic ferromagnetism of O-terminated ZnO (0001) surfaces, and is not the result of the adsorption of $NH_3$. For $(10\bar{1}0)$ surfaces with Zn DBs passivated by F, Cl, and OH, and for F-ZnONWs, the FM state is the most stable whereas the NM state is the most unstable (Table S2 in the Supporting Information). For $H_2N$-ZnO $(10\bar{1}0)$, however, the ground state is an AFM state, 104.83 meV more favorable than its corresponding FM state. This is an AFM semiconductor with an indirect gap of 0.16 eV, which differs from the results of ZnO nanoribbons because of the different geometrical structures.[10] The total magnetic moment of the FM configuration for F-, HO-, and $H_2N$-ZnO $(10\bar{1}0)$ surfaces is 1.0 $\mu_B$ unit cell$^{-1}$, whereas it is

  

only 0.53 $\mu_B$ unit cell$^{-1}$ for Cl-ZnO (10$\bar{1}$0). The magnetic moment induced by each Cl atom is improved when the dimensions of ZnO decrease from two to one. The total magnetic moments for triangular, quadrangular, and hexangular F-, Cl-, and HO-ZnONWs are 9.0, 10.0, and 12.0 $\mu_B$ unit cell$^{-1}$, respectively. For both F-ZnONW-1 and F-ZnONW-2, the total magnetic moments are 6.0 $\mu_B$ unit cell$^{-1}$. Therefore, the magnetic moments in ZnONWs can be altered by changing the coverage of passivants as well as the diameter and length. For the (1×2) F-ZnO (10$\bar{1}$0) surface, the FM state is 20.81 meV (10.41 meV F$^{-1}$) lower in energy than the AFM state, whereas the FM state is 266.39 meV (22.20 meV F$^{-1}$) lower in energy than the AFM state for the hexangular F-ZnONW. This indicates that when the dimensions of ZnO decrease from two to one, FM stability is improved and the Curie temperature ($T_c$) increases. Thus, ferromagnetism above room temperature could be expected for F-ZnONWs.

To further investigate the distribution of the magnetic moment, we calculated the magnetic moment on each atom, as displayed in Table 1. All Zn atoms of the studied system carry negligible magnetic moments (not shown in Table 1). For F-ZnO (10$\bar{1}$0), the magnetic moment mainly stems from the surface O (0.43 $\mu_B$) and F (0.16 $\mu_B$). The situation is the same for F-ZnONWs, but the individual magnetic moments of surface O atoms for F-ZnO are enhanced when the dimensions of ZnO decrease from two to one. For F-ZnONW-2, the surface O(s) atoms of O(s)–Zn(F) parallel to the <0001> direction have the largest local magnetic moment (0.32 $\mu_B$), whereas the other surface O atoms, the subsurface O(sub) atoms, and the F atoms carry magnetic moments 0.17 $\mu_B$, 0.11~0.12 $\mu_B$, and 0.11 $\mu_B$, respectively. For Cl-ZnONW, the magnetic moment stems mainly from the Cl atoms, whereas the O atom on the surface layer has the second largest local magnetic moment. For HO-ZnO (10$\bar{1}$0), both the O on OH and the surface oxygen atoms carry a magnetic moment of 0.31 $\mu_B$. For (2×1) $H_2N$-ZnO (10$\bar{1}$0), the magnetic moments of the AFM state are located mainly on the N atoms (one is 0.42 $\mu_B$, the other is −0.42 $\mu_B$). These results indicate that different passivants lead to different magnetic moment distributions. The higher electronegativity of F creates more holes in the corresponding surface O atoms and causes them to carry the largest magnetic moments; for the Cl, OH, and $NH_2$ passivants, the Cl, O, and N carry the largest magnetic moments due to their lower electronegativity.

Table 1. The magnetic moment ($M$) distributions of X-ZnO (10$\bar{1}$0) and X-ZnONW.

| | $M$ [$\mu_B$] | | |
|---|---|---|---|
| | F/Cl/N/O(H) | O(s)[a] | O(sub)[b] |
| F-ZnO (10$\bar{1}$0) | 0.16 | 0.43 | 0.10 |
| triangular F-ZnONW | 0.17~0.19 | 0.51~0.59 | 0.20~0.26 |
| quadrangular F-ZnONW | 0.15~0.18 | 0.50~0.56 | 0.19~0.21 |
| hexangular F-ZnONW | 0.16 | 0.48~0.49 | 0.13~0.20 |
| F-ZnONW-2 | 0.11 | 0.32, 0.17 | 0.11~0.12 |
| hexangular Cl-ZnONW | 0.40 | 0.26~0.28 | 0.13~0.14 |
| HO-ZnO (10$\bar{1}$0) | 0.31 | 0.31 | 0.06 |
| (2×1) $H_2N$-ZnO (10$\bar{1}$0) | 0.42, −0.42 | 0.09, −0.09 | 0.08, −0.08 |

[a] Surface oxygen atoms. [b] The oxygen atoms in the subsurface layer.

An explanation of the origin of the magnetic properties can be given from the view point of Bader charge analysis and electronic structures. The change in the coordination of surface atoms for the bare wires and the 50% $NH_3$ passivation weakly affects the charge distribution of Zn and O atoms (Table S5 in the Supporting Information), so no magnetism is induced. Because the surface Zn atoms are passivated by F, Cl, OH, and $NH_2$, the Zn atom transfers part of its charge to F, Cl, N, and O, and the charge transfer to the neighboring O atoms decreases, creating holes in the O 2p orbitals and resulting in magnetic systems in which the 2p electrons in O, N, and F and the 3p electrons in the Cl sites are spin polarized (Table S5 in the Supporting Information). The large electronegativity of F leads to the largest charge transfer, leaving more holes in the O 2p orbitals. Consequently, these polarized charge carriers localized around the O, N, Cl, and F sites mediate the long-range magnetic coupling.

The generalized gradient approximation (GGA) calculations show that bare ZnONWs are non-magnetic semiconductors, and all ZnONWs with surface Zn atoms passivated by F, Cl, and OH are half-metals. It has, however, been argued that the spin-dependent GGA may fail to properly represent localized 3d electrons. It may be that on-site repulsive Coulomb interaction destroys the HM state. Therefore, we carried out GGA+$U$ calculations to examine the effect of on-site Coulomb repulsion and found the bare hexangular ZnONW to have a direct band gap (2.18 eV) at Γ by using GGA+$U$. After on-site Coulomb $U$ correlated correction, the F-ZnO NWs still showed HM behavior.

The analysis of electronic structures indicates that for the bare wires the top of the valence bands is composed mainly of O 2p states, whereas the bottom of the conduction bands is mainly contributed by Zn 4s states. The partial surface passivation causes great changes in the electronic structures of ZnO. Figure 2 displays the band structures for the F-ZnO (10$\bar{1}$0) surface and F-ZnONWs by GGA+$U$ calculations, and Figure 3 shows the total density of states (TDOS) and partial DOS (PDOS) for F-ZnO (10$\bar{1}$0) and hexangular F-ZnONWs. Compared with F-ZnO (10$\bar{1}$0), the FM configurations of F-ZnONWs have more split bands above and below the Fermi level. For F-ZnONWs, there are two spin-down bands crossing the Fermi level to lead to an HM system with charge-compensating holes of well-defined spin polarization. In addition to these, there are 8, 9, and 11 spin-down bands just above the Fermi level for the triangular, quadrangular, and hexangular F-ZnONWs, respectively. This indicates that holes mediate FM coupling. The band structure of spin-up shows that the direct band gaps are 2.44, 4.43, 4.16, and 3.57 eV for F-ZnO (10$\bar{1}$0) surface, triangular, quadrangular, and hexangular F-ZnONWs, respectively, which indi-

  

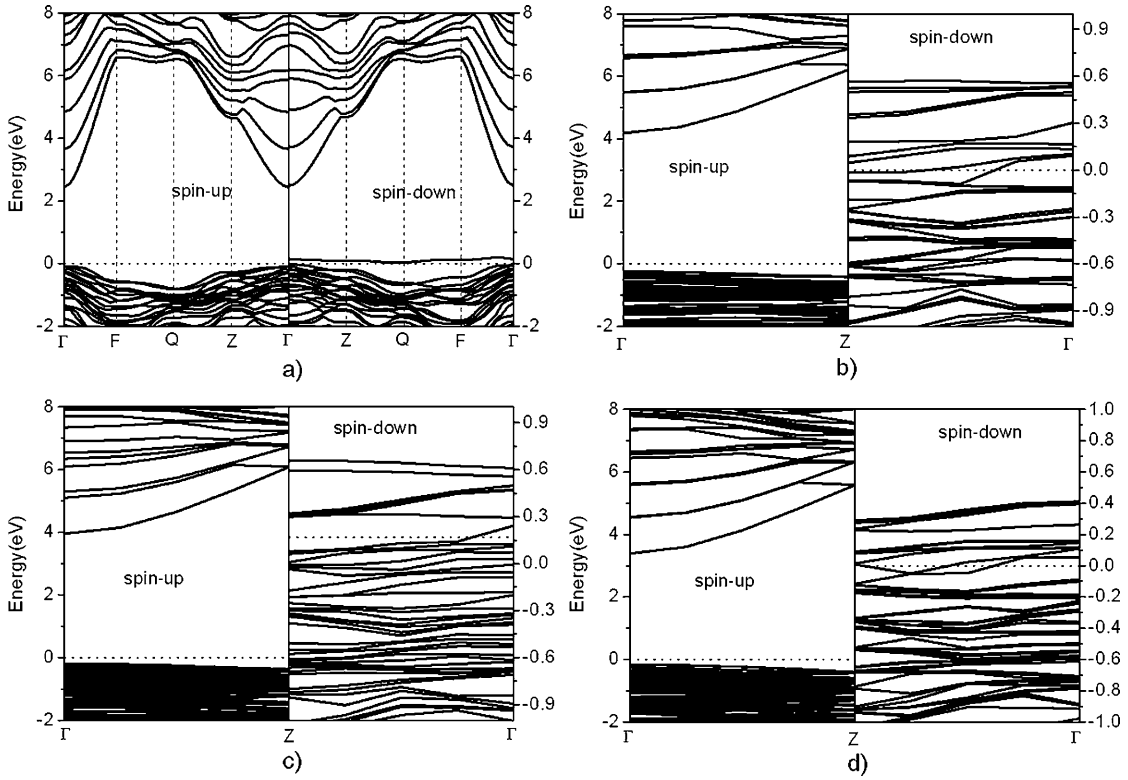


Figure 2. The GGA+$U$ band structures for the FM configurations of a) F-ZnO ($10\bar{1}0$), b) triangular F-ZnONW, c) quadrangular F-ZnONW, and d) hexangular F-ZnONW.

cate the quantum confinement effects on the band gap. Figure 3 shows that the magnetic moments are contributed mainly by the bands near the Fermi level, which are mostly from the surface O 2p orbitals with a mixing of F 2p and subsurface O 2p orbitals. The bands near the Fermi level also oscillate, which shows that the p orbitals are delocalized and could promote long-range exchange coupling interactions. The p orbital characteristics of spin density differ completely from the origin of magnetism in TM-doped ZnO, in which the localized 3d orbitals of dopants contribute to the observed magnetism. That is to say, the passivation of F atoms at Zn sites introduces holes in the O 2p states, which couple the nearest O 2p and F 2p states by p–p interactions because these interactions are relatively long-ranged. This long-range coupling pushes the minority p–p mixed state upward and the opposite spin state downward, thus leading to metallicity in the spin-down direction and lowering the total energy of the system.

In conclusion, we predict that ZnO surfaces and nanowires offer interesting magnetic properties when only the surface Zn atoms are chemically decorated. The partial surface passivation of the surface zinc bonds with oxygen DBs causes redistribution of charges in Zn, O, and surface passivants, inducing magnetism. The magnetic moments of ZnONWs can be modified with the coverage of passivants as well as diameter and length. In particular, the ZnONWs with zinc DBs partially or fully passivated by F acquire half-metallic behavior from DFT+$U$ calculations. The FM stability is improved when the dimensions of ZnO decrease from two to one. Compared with conventional 3d TM cation-doped DMSs, non-TM surface adsorption provides a possible way to resolve the clustering problem of magnetic elements and opens up another route for producing potentially useful DMSs.

## Computational Methods

We performed calculations by using both spin-polarized and spin-unpolarized DFT within the generalized gradient approximation (GGA) as implemented in the Vienna ab initio simulation package (VASP).[12] We adopted the Perdew and Wang (PW91) form[13] of the GGA with the projected augmented wave (PAW)[14] potentials, and also employed the GGA+$U$[15] method to explore the effect of Coulomb correlation $U$ on the ferromagnetic stability, with $U=7.8$ as described in earlier works.[1h,16] More computational details are described in the Supporting Information.

## Acknowledgements

The work described in this paper was supported by grants from the Research Grants Council of the Hong Kong Special Administrative Region, China (CityU3/CRF/08, CityU 110209).

  

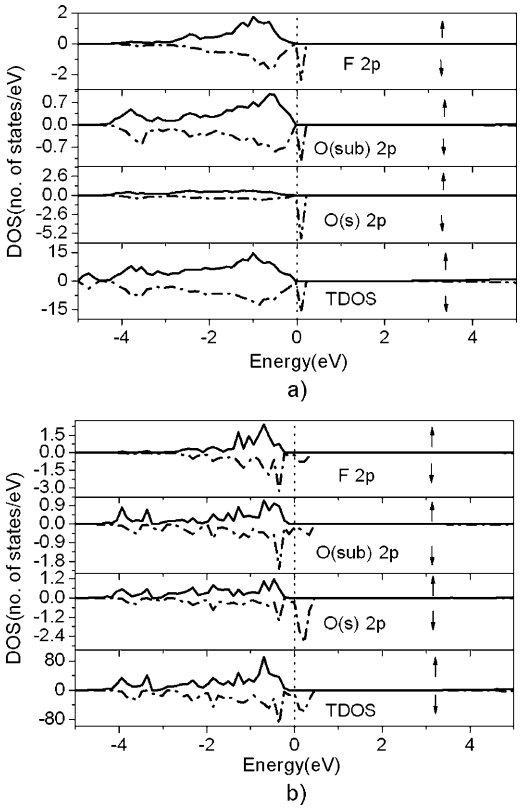


Figure 3. The GGA+$U$ TDOS and PDOS for a) F-ZnO ($10\bar{1}0$) and b) hexangular F-ZnONWs. O(s) and O(sub) represent the surface and subsurface O atoms, respectively. The Fermi level is shown as a dashed line. The up and down arrows denote spin-up and spin-down, respectively.

**Keywords:** charge transfer · half-metal · magnetic properties · surface passivation · zinc oxide

[1] a) S. A. Wolf, D. D. Awschalom, R. A. Buhrman, J. M. Daughton, S. V. Molnár, M. L. Roukes, A. Y. Chtchelkanova, D. M. Treger, *Science* **2001**, *294*, 1488; b) H. Jeon, J. Ding, A. V. Nurmikko, H. Luo, N. Samarth, J. Furdyna, *Appl. Phys. Lett.* **1991**, *59*, 1293; c) C. T. Walker, J. M. DePuydt, M. A. Haase, J. Qiu, H. Cheng, *Physica B+C* **1993**, *185*, 27.

[2] a) H. Xu, A. L. Rosa, T. Frauenheim, R. Q. Zhang, S. T. Lee, *Appl. Phys. Lett.* **2007**, *91*, 031914; b) H. Xu, W. Fan, A. L. Rosa, R. Q. Zhang, T. Frauenheim, *Phys. Rev. B* **2009**, *79*, 073402.

[3] S. P. Huang, H. Xu, I. Bello, R. Q. Zhang, *J. Phys. Chem. C* **2010**, *114*, 8861.

[4] D. C. Kundaliya, S. B. Ogale, S. E. Lofland, S. Dhar, C. J. Metting, S. R. Shinde, Z. Ma, B. Varughese, K. V. Ramanujachari, L. Salamanca-Riba, T. Venkatesan, *Nat. Mater.* **2004**, *3*, 709.

[5] a) C. F. Yu, T. J. Lin, S. J. Sun, H. Chou, *J. Phys. D* **2007**, *40*, 6497; b) H. Pan, J. B. Yi, L. Shen, R. Q. Wu, J. H. Yang, J. Y. Lin, Y. P. Feng, J. Ding, L. H. Van, J. H. Yin, *Phys. Rev. Lett.* **2007**, *99*, 127201; c) N. H. Hong, J. Sakai, V. Brize, *J. Phys. Condens. Matter* **2007**, *19*, 036219; d) L. Shen, R. Q. Wu, H. Pan, G. W. Peng, M. Yang, Z. D. Sha, Y. P. Feng, *Phys. Rev. B* **2008**, *78*, 073306; e) B. J. Nagare, S. Chacko, D. G. Kanhere, *J. Phys. Chem. A* **2010**, *114*, 2689; f) Q. Wang, Q. Sun, G. Chen, Y. Kawazoe, P. Jena, *Phys. Rev. B* **2008**, *77*, 205411; g) A. L. Schoenhalz, J. T. Arantes, A. Fazzio, G. M. Dalpian, *Appl. Phys. Lett.* **2009**, *94*, 162503.

[6] C. S. Guo, L. B. Luo, G. D. Yuan, X. B. Yang, R. Q. Zhang, W. J. Zhang, S. T. Lee, *Angew. Chem.* **2009**, *121*, 10080; *Angew. Chem. Int. Ed.* **2009**, *48*, 9896.

[7] a) M. A. Garcia, J. M. Merino, E. Fernández Pinel, A. Quesada, J. de La Venta, M. L. Ruíz González, G. R. Castro, P. Crespo, J. Llopis, J. M. González-Calbet, A. Hernando, *Nano Lett.* **2007**, *7*, 1489; b) Q. Wang, Q. Sun, P. Jena, *J. Chem. Phys.* **2008**, *129*, 164714; c) E. Z. Liu, J. Z. Jiang, *J. Phys. Chem. C* **2009**, *113*, 16116; d) J. F. Liu, E. Z. Liu, H. Wang, N. H. Su, J. Qi, J. Z. Jiang, *Nanotechnology* **2009**, *20*, 165702; e) S. Z. Deng, H. M. Fan, M. Wang, M. R. Zheng, J. B. Yi, R. Q. Wu, H. R. Tan, C. H. Sow, J. Ding, Y. P. Feng, K. P. Loh, *ACS Nano* **2010**, *4*, 495.

[8] E.-C. Lee, K. J. Chang, *Phys. Rev. B* **2004**, *69*, 085205.

[9] a) S. J. Hu, S. S. Yan, M. W. Zhao, L. M. Mei, *Phys. Rev. B* **2006**, *73*, 245205; b) S.-W. Lim, D.-K. Hwang, J.-M. Myoung, *Solid State Commun.* **2003**, *125*, 231.

[10] Q. Chen, L. Y. Zhu, J. L. Wang, *Appl. Phys. Lett.* **2009**, *95*, 133116.

[11] J. Winterlik, G. H. Fecher, C. Felser, C. Mühle, M. Jansen, *J. Am. Chem. Soc.* **2007**, *129*, 6990.

[12] G. Kresse, J. Furthmüller, *Phys. Rev. B* **1996**, *54*, 11169.

[13] J. P. Perdew, Y. Wang, *Phys. Rev. B* **1992**, *45*, 13244.

[14] P. E. Blöchl, *Phys. Rev. B* **1994**, *50*, 17953.

[15] S. L. Dudarev, G. A. Botton, S. Y. Savrasov, C. J. Humphreys, A. P. Sutton, *Phys. Rev. B* **1998**, *57*, 1505.

[16] P. Erhart, K. Albe, A. Klein, *Phys. Rev. B* **2006**, *73*, 205203.

Received: May 1, 2010
Published online: October 13, 2010

  